EFFECT OF SINE-SQUARED THERMAL BOUNDARY CONDITION ON AUGMENTATION OF HEAT TRANSFER IN A TRIANGULAR SOLAR COLLECTOR FILLED WITH DIFFERENT NANOFLUIDS

M. M. Rahman[1,2], S. Saha[3], S. Mojumder[3], A. G. Naim[1], R. Saidur[4], and Talaat A. Ibrahim[5,6]

[1]*Universiti Brunei Darussalam Mathematical and Computing Sciences Group, Faculty of Science, Darussalam, Brunei*

[2]*Department of Mathematics, Bangladesh University of Engineering and Technology, Dhaka, Bangladesh*

[3]*Department of Mechanical Engineering, Bangladesh University of Engineering and Technology, Dhaka, Bangladesh*

[4]*Department of Mechanical Engineering, Faculty of Engineering, University of Malaya, Kuala Lumpur, Malaysia*

[5]*Vice Presidency for Projects, King Saud University, Riyadh, Saudi Arabia*

[6]*Mechanical Power Department, Faculty of Engineering-Mattaria, Helwan University, Cairo, Egypt*

Numerical study of heat transfer phenomena has become a major field of research nowadays. In engineering applications, different boundary conditions arise which have various effects on heat transfer characteristics. For the present work, a triangular-shape cavity has been analyzed for the sine-squared thermal boundary condition which is common in practical cases. The augmentation of heat transfer has been done by introducing a nanofluid inside the cavity. Different solid volume fractions ($\phi = 0, 0.05, 0.1, 0.2$) of water-CuO, water-Al_2O_3, and water-TiO_2 nanofluid have been tested for the cavity with a wide range of Rayleigh number ($\mathrm{Ra} = 10^5$–10^8) and for dimensionless time ($\tau = 0.1$ to 1). The Galerkin weighted residual finite-element method has been applied for the numerical solution, and numerical accuracy has been checked by code validation. The heat transfer augmentation for different nanofluids has been done in the light of local (Nu_L) and overall Nusselt number (Nu_{av}), and the results have been presented with streamline, isotherm, and related contours, in graphs and charts. It has been found that variable boundary condition has significant effect on flow and thermal fields and increase of solid volume fraction enhances the heat transfer.

Received 28 September 2014; accepted 10 November 2014.

Address correspondence to M. M. Rahman, Universiti Brunei Darussalam Mathematical and Computing Sciences Group, Faculty of Science, BE 1410, Brunei. E-mail: mustafizur.rahman@ubd.edu.bn

Color versions of one or more of the figures in the article can be found online at www.tandfonline.com/unhb.

NOMENCLATURE

c_p	specific heat, J/kg k	α	thermal diffusivity, m^2/s
g	gravitational acceleration, m/s^2	β	thermal expansion coefficient, K^{-1}
k	thermal conductivity, W/m k	Γ_φ	diffusion term in Eq. (1)
L	length of the enclosure, m	θ	nondimensional temperature
Nu	Nusselt number	μ	dynamic viscosity, kg/m s
p	dimensional pressure, $kg/m\,s^2$	ν	kinematic viscosity, m^2/s^{-1}
P	dimensionless pressure	τ	dimensionless time
Pr	Prandtl number	ρ	density, kg/m^3
Ra	Rayleigh number	ϕ	solid volume fraction
S_φ	source term in Eq. (1)	ψ	streamfunction
t	dimensional time, s	φ	general dependent variable
T	fluid temperature, K		
u	horizontal velocity component, m/s	**Subscripts**	
U	dimensionless horizontal velocity component	av	average
		c	cold
v	vertical velocity component, m/s	f	fluid
V	dimensionless vertical velocity component	h	heat source
		L	local
x	horizontal coordinate, m	nf	nanofluid
X	dimensionless horizontal coordinate	max	maximum
y	vertical coordinate, m	min	minimum
Y	dimensionless vertical coordinate	s	solid nanoparticle

1. INTRODUCTION

Augmentation of heat transfer using nanofluids is a cutting-edge research topic. From different studies, it has been proved that nanofluid has great potential to serve the purpose of heat transfer to a great extent. Apart from this, it has numerous applications in different fields of science and technology such as electronics cooling, chemical processing industries, food processing industries, space heating, solar thermal collectors, desalination technology, and so on [1–5]. Basically, natural convection plays a significant role in nanofluid-augmented heat transfer. Martin et al. [6] analyzed the laminar natural convection in a triangular enclosure and showed the effect of aspect ratio and Grashof number for different boundary conditions. Rahman et al. [7] studied the natural-convection effects on heat and mass transfer in a curvilinear triangular cavity and reported that Lewis number, Sherwood number, and buoyancy ratio have significant effects on heat and mass transfer. The authors reported that increment of buoyancy ratio enhances heat and mass transfer, while increment of Lewis number decreases heat transfer but enhances mass transfer. Using the Bejan heatline concept, Basak et al. [8] visualized the heat flow due to natural convection and concluded that increment of Rayleigh number makes the convection mode of heat transfer stronger. However, this effect is not significant for higher Prandtl (Pr) number. Koca et al. [9] studied the effect of Prandtl number on natural convection in a triangular enclosure with a localized heater from the bottom and reported that Prandtl number has a significant effect on heat transfer.

Nanofluids have been introduced as conventional fluids that have limitations in their thermophysical properties. The improved thermo-physical properties of the nanoparticles that are suspended in the base fluid are the main reason behind better heat transfer. Different types of nanoparticles are suspended for preparing nanofluids such as metals, metal oxides, carbon substances, etc. Though different types of nanofluid are available, very few of them are commercially viable. Among the commercial nanofluids, CuO-water, Al_2O_3-water, and TiO_2-water are used extensively nowadays. Different solid volume fractions of this suspended nanoparticle alter the consequent heat transfer. Different types of geometry have been studied by introducing nanofluids into them. Among those geometries, square [10–12], rectangular [13], and trapezoidal [14–16] are the common ones. The triangular type of cavity has been given rather less attention, though this type of cavity has many engineering applications. Sivsankaran and Pan [17] studied the natural convection of nanofluids in a cavity with a sinusoidal boundary condition along with nonuniform temperature distributions and reported that amplitude ratio, solid volume fraction, and Rayleigh number have noteworthy effects on heat transfer. Rahman et al. [18] studied the heat transfer characteristic in an inclined lid-driven triangular enclosure and found that the fluid flow and heat transfer pattern are strongly dependent on the solid volume fraction of the nanofluid. Nasrin et al. [19] studied the combined-convection flow in a triangular wavy chamber for nanofluids and observed the effect of viscosity models. The authors reported effects of Reynolds number and Richardson number along with solid volume fraction on heat transfer characteristics. Yu et al. [20] studied the transient convection for different water-based nanofluids in an isosceles triangular cavity having a heated bottom and showed the effect of Grashof number on heat transfer. Rahman et al. [21] studied the effect of different nanofluids in a triangular-shape solar thermal collector and reported that heat transfer can be increased up to 24.28% for 10% of the solid volume fraction of the nanofluid. Ghasemi and Aminossadati [22] studied mixed convection for a triangular cavity filled with nanofluid and claimed that the increase of nanoparticles enhances the heat transfer. More related studies for the enhancement of heat transfer using nanofluids can be found in recent literature [23–28]. From the aforementioned review, it is evident that heat transfer may be enhanced by increasing solid volume fraction, Rayleigh number, and Grashof number while decreasing Lewis number.

Boundary conditions are pertinent parameters which are modeled based on the physical manifestation of that particular problem in real life. Different types of boundary condition have tried in different literatures reports. Among them, a simply heated wall, nonuniform heating, and linearly varying boundary conditions have been studied extensively. The sinusoidally heated boundary condition is drawing keen attention due to its frequent occurrence in engineering fields. The effect of variable boundary conditions in a porous right-angled triangular cavity has been studied by Basak et al. [29], and they reported the effect of variable boundary conditions on heat transfer. Bilgen and Yedder [30] studied the effect of a sinusoidal temperature profile on the wall for natural convection. Basak and Chamakha [31] studied a square cavity filled with nanofluid for different boundary conditions and analyzed the solutions for different pertinent parameters, showing that heat transfer is influenced by solid volume fraction and the boundary condition. Cheong et al. [32] studied the effect of aspect ratio in a square cavity for sinusoidal boundary condition and showed that the convective flow pattern is affected significantly by the boundary condition. More related literature [33–37] for sinusoidal thermal boundary condition reveals that this sort of boundary condition has tremendous influence on heat transfer.

Nanofluids are commonly used in solar collectors to improve the efficiency of the collector. Different types of solar collector have been studied [21, 38, 39] for different available nanofluids. Throughout this article, a triangular-shaped solar thermal collector has been modeled. Boundary conditions are so modeled so that they resemble the practical scenario. To the best knowledge of the authors, a triangular solar thermal collector filled with different nanofluids and sinusoidally heated from the bottom has not been analyzed yet. The challenge of augmentation of heat transfer in solar thermal collectors can be met with this model. The study has been carried out numerically with an accurate numerical procedure, and the related results are shown using streamlines, isotherms, and related graphs and charts. The results reveal that the augmentation of heat transfer is possible by introducing nanofluid inside the collector.

2. PROBLEM FORMULATION

2.1. Physical Modeling

The details of the problem are presented in Figure 1. In the figure, a triangular-shape geometry of base length L and height of half of the base length L is shown. The entire cavity is filled with nanofluid to increase the heat transfer inside the cavity. A well-defined coordinate system has been fixed, and gravity is working along the negative Y axis. The inclined walls of the cavity are kept at low temperature ($T = T_c$), and the horizontal wall is kept at a sinusoidally varying temperature $[T = T_c + (T_h - T_c)A\sin^2(\underline{K}x)]$. Here A is the amplitude of the wave and $\underline{K}$ is the wave number, given by $\underline{K} = 2\pi/L$. Different types and concentrations ($\phi = 0$, 0.05, 0.1, 0.2) of nanofluid, such as water-CuO, water-Al_2O_3, and water-TiO_2, have been studied for this geometry. Radiation effects, and viscous dissipation with internal heat generation have been neglected. Basically, this type of cavity is modeled as a solar collector of which the inclined walls are the glass covers and the sinusoidally heated wall is the collector plate. The temperature of the glass cover is very low relative to that of the base horizontal collector plate.

2.2. Mathematical Modeling

A set of governing equations has been formed assuming that the nanofluid is a Newtonian fluid and the flow is unsteady and laminar. The incompressible Navier-Stokes equation has been applied for the two-dimensional flow. The Boussinesq approximation has been applied to consider the density variation. Conservation laws of mass, momentum, and energy control the system behavior, which has been modeled through the accompanying mathematical equations. From the above-stated assumptions of the two-dimensional fluid flow field we can write

$$\frac{\partial(\varphi)}{\partial\tau} + \frac{\partial(U\varphi)}{\partial X} + \frac{\partial(V\varphi)}{\partial Y} = \frac{\partial}{\partial X}\left(\Gamma_\varphi \frac{\partial\varphi}{\partial X}\right) + \frac{\partial}{\partial Y}\left(\Gamma_\varphi \frac{\partial\varphi}{\partial Y}\right) + S_\varphi \tag{1}$$

Here, dependent nondimensional variables are designated by φ, and the corresponding diffusion and source term are defined by Γ_φ and S_φ, respectively; they are summarized in Table 1.

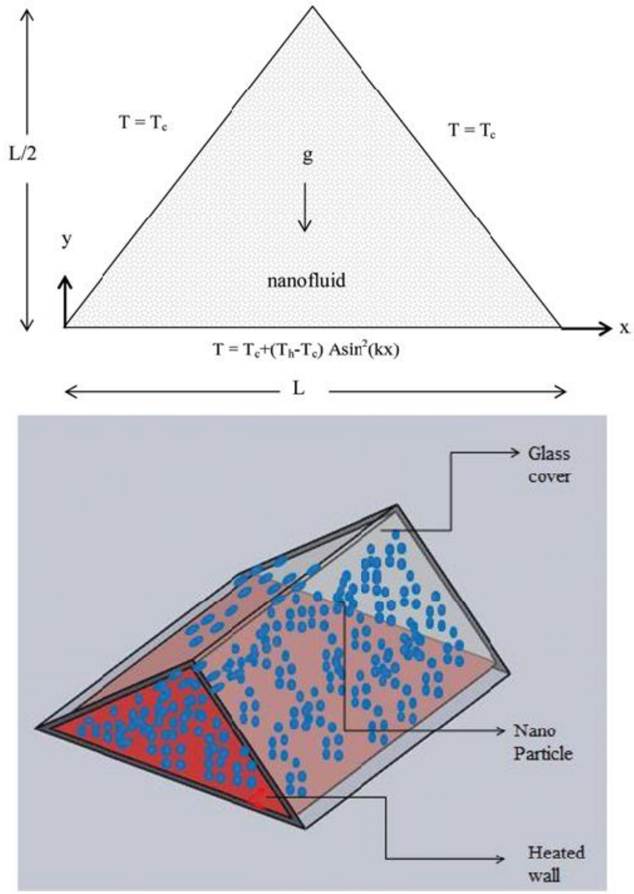

Figure 1. Schematic view of the triangular-shaped cavity with the boundary conditions.

The density of the nanofluid, which is assumed to be constant, can be expressed as

$$\rho_{\mathrm{nf}} = (1 - \phi)\rho_f + \phi\rho_s \tag{2}$$

Table 1. Summary of governing nondimensional equations [37]

Equation	φ	Γ_φ	S_φ
Continuity	1	0	0
U momentum	*U*	$\mu_{\mathrm{nf}}/\rho_{\mathrm{nf}}\alpha_f$	$-\partial P/\partial X$
V momentum	*V*	$\mu_{\mathrm{nf}}/\rho_{\mathrm{nf}}\alpha_f$	$-\partial P/\partial Y + [(\rho\beta)_{\mathrm{nf}}/(\rho_{\mathrm{nf}}\beta_f)]\mathrm{Ra}\,\mathrm{Pr}\,\theta$
Energy	θ	$\alpha_{\mathrm{nf}}/\alpha_f$	0

In the above equation, the solid volume fraction (ϕ) has significant effect on heat transfer, and the thermal diffusivity of the nanofluid, which is quite different from that of a conventional fluid, can be expressed as

$$\alpha_{\text{nf}} = \frac{k_{\text{nf}}}{(\rho c_p)_{\text{nf}}} \tag{3}$$

where the heat capacitance of the nanofluid $(\rho c_p)_{\text{nf}}$ can be found by

$$(\rho c_p)_{\text{nf}} = (1-\phi)(\rho c_p)_f + \phi(\rho c_p)_s \tag{4}$$

In addition, the thermal expansion coefficient $(\rho\beta)_{\text{nf}}$ of the nanofluid is

$$(\rho\beta)_{\text{nf}} = (1-\phi)(\rho\beta)_f + \phi(\rho\beta)_s \tag{5}$$

Moreover, the dynamic viscosity (μ_{nf}) of the nanofluid can be expressed as

$$\mu_{\text{nf}} = \frac{\mu_f}{(1-\phi)^{2.5}} \tag{6}$$

The effective thermal conductivity of the nanofluid can be described as

$$\frac{k_{\text{nf}}}{k_f} = \frac{k_s + 2k_f - 2\phi(k_f - k_s)}{k_s + 2k_f + \phi(k_f - k_s)} \tag{7}$$

where the thermal conductivity of the nanoparticles is k_s and the thermal conductivity of the base fluid is k_f.

Scaling which has been carried out to obtain the nondimensional governing equations is presented in Eq. (8):

$$\begin{gathered} X = \frac{x}{L} \quad Y = \frac{y}{L} \quad \tau = \frac{\alpha_f t}{L^2} \quad U = \frac{uL}{\alpha_f} \quad V = \frac{vL}{\alpha_f} \\ P = \frac{(p + \rho_f g y)L^2}{\rho_{nf}\ \alpha_f^2} \quad \theta = \frac{(T - T_c)}{(T_h - T_c)}\ \mathrm{Ra} = \frac{g\beta_f L^3 (T_h - T_c)}{\alpha_f \nu_f} \quad \Pr = \frac{\nu_f}{\alpha_f} \end{gathered} \tag{8}$$

In the above equations, θ is nondimensional temperature. Rayleigh number and Prandtl number are designated by Ra and Pr, respectively.

Initial and boundary conditions in dimensionless form for the present problems can be defined by

$$\begin{aligned} &\tau = 0 \\ &\text{Entire domain}: U = V = 0, \theta = 0 \\ &\tau > 0 \end{aligned} \tag{9a}$$

$$\text{On the base wall}: U = V = 0, \theta = A\ \sin^2(2\pi X) \tag{9b}$$

Table 2. Thermophysical properties of water and nanoparticles [21]

Property	Water	Cu	Al_2O_3	TiO_2
c_p (J/kg K)	4,179	385	765	686.2
ρ (kg/m^3)	997.1	8,933	3,970	4,250
K (W/mK)	0.613	400	40	8.9538
β (1/K)	2.1×10^{-4}	1.67×10^{-5}	0.85×10^{-5}	0.9×10^{-5}

$$\text{On the side walls : } U = V = 0, \theta = 0 \tag{9c}$$

Average Nusselt number has been evaluated for the bottom horizontal heated surface and calculated from the following expression:

$$\mathrm{Nu}_{\mathrm{av}} = -\frac{k_{\mathrm{nf}}}{k_f} \int_0^1 \frac{\partial \theta}{\partial Y} \, dX \tag{10}$$

Streamfunction ψ is a mathematical trick which has been introduced to represent the fluid motion. Streamfunction has been defined from velocity components U and V. The relation between the streamfunction and the velocity component for a two-dimensional flow is given by

$$U = \frac{\partial \psi}{\partial Y} \quad V = -\frac{\partial \psi}{\partial X} \tag{11}$$

2.3. Thermophysical Properties of the Nanofluid

Different types of nanofluid have been studied for the present work, and most of them are highly used in the commercial case due to their availability and economic considerations. Analysis has been performed for water-CuO, water-Al_2O_3, and water-TiO_2 nanofluids. These nanofluids are being used extensively commercially due to their improved thermophysical properties. The thermophysical properties of these nanofluids are presented in Table 2 [21]. Beside these nanofluids, other new nanofluids are now coming into focus. Among them, graphene-water, CNT (carbon nanotube)-water, diamond-water, and Ag-water are very common, but these nanofluids are costly. The solid volume fraction of the nanofluid plays a significant role in heat transfer augmentation, and heat transfer using nanofluids is a very complex mechanism.

3. NUMERICAL PROCEDURE AND CODE VALIDATION

The Galerkin weighted residual finite element method (FEM) has been applied to the present problem to obtain a numerical solution. The Boussinesq approximation has been applied to consider variation of density. The entire geometry has been discretized into several elements using a triangular mesh method. Governing equations with initial and boundary conditions have been applied to these elements

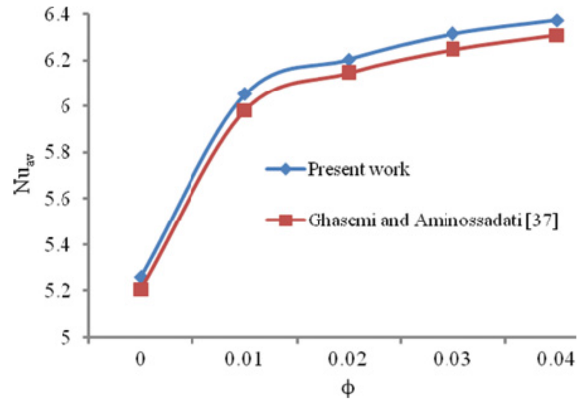

Figure 2. Validation of the present code against the results of Ghasemi and Aminossadati [37].

to obtain a set of algebraic equations. Iteration technique has been applied to solve these algebraic linear equations parametrically for the entire domain applying proper boundary condition. The convergeuce criterion of the numerical solution along with error estimation has been set to $|\varphi^{m+1} - \varphi^{m}| \leq 10^{-5}$, where φ is the general dependent variable and m is the number of iteration.

Code validation of the present work has been done to check the accuracy of the present code with the established literature. The details of the code validation are presented in Figure 2. The present work is compared with that of Ghasemi and Aminossadati [37] in light of average Nusselt number. From the figure, it is evident that the present work is completely in par with the previously established literature. So, the present numerical code and solution procedure are completely reliable, and so is the numerical solution.

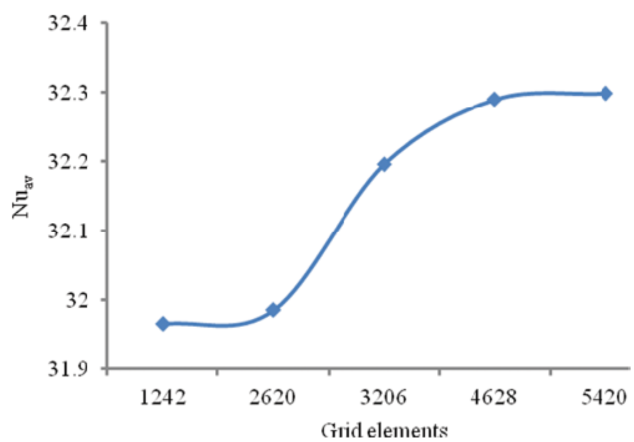

Figure 3. Grid independence study with $\tau = 0.1$, $\phi = 0.05$, and $Ra = 10^8$ for CuO-water.

4. GRID INDEPENDENCE TEST

A grid independence test for the present problem has been performed for different element numbers to test the numerical accuracy of the present work. When the grid element number is increased, the numerical solution becomes more accurate but, due to computational limitations, obtaining an independent grid can save time and computational effort. The result of the grid independence test is presented in the Figure 3. Grid independence study has been carried out for dimensionless time $\tau = 0.1$, solid volume fraction $\phi = 0.05$, and $Ra = 10^8$ with CuO-water nanofluid. It has been performed on the basis of average Nusselt number. Different grids of element numbers 1,242, 2,620, 3,206, 4,628, and 5,420 have been checked, and it is clear from the figure that for the element numbers 1,242 and 2,620, the Nusselt number does not vary. Again, with the addition of more elements, for example, at 3,206, Nusselt number changes significantly. When the element number is set to 4,628, it becomes more or less constant for further increment of elements (such as 5,420). So, the entire solution process becomes independent of the grid when the element number is set to 4,628 for the numerical solution. Thus, a grid having 4,628 elements

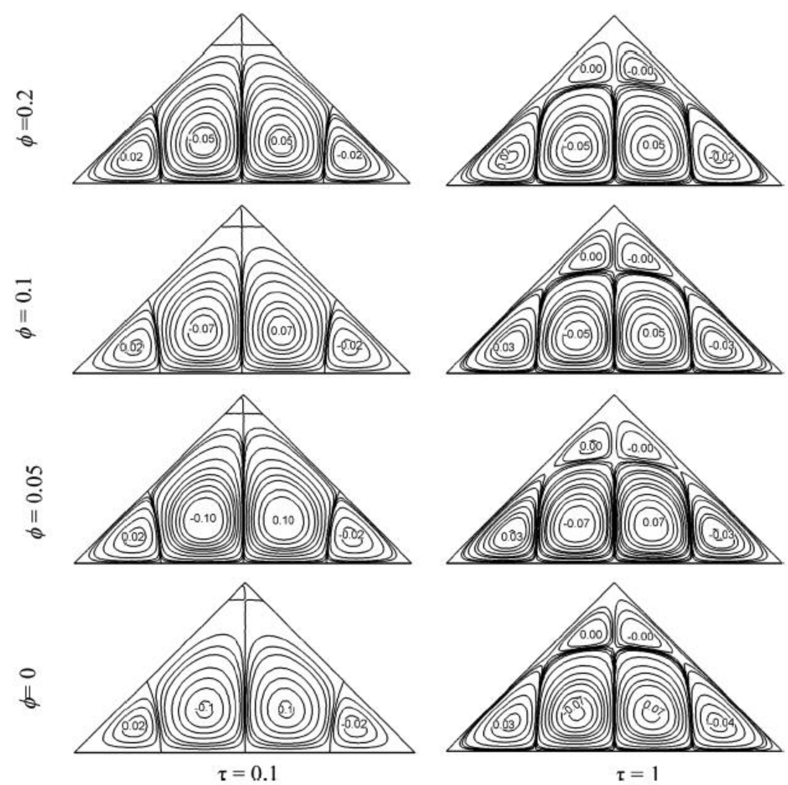

Figure 4. Effect of solid volume fraction on streamlines for the selected values of τ with $Ra = 10^5$ (CuO-water).

has been considered as an independent grid, and the whole numerical simulation is performed taking it as the grid element distribution.

5. RESULTS AND DISCUSSION

In the present article, numerical calculations were carried out with the help of finite-element analysis. A set of differential equations was solved by a sophisticated algorithm which has been verified. Results are presented through streamline and isotherm contours along with necessary plots. The present research deals with a special kind of boundary condition which has not been explored widely but is of immense practical importance. So, effort was given to include in the research output as much detail as possible.

5.1. Effect of Solid Volume Fraction on Streamline Contours

Figures 4–7 exhibit the effect of solid volume fraction of nanoparticles in the base fluid on the streamline contours at different values of τ and Rayleigh number. From the nondimensional parameters' definitions, it is evident that higher values of

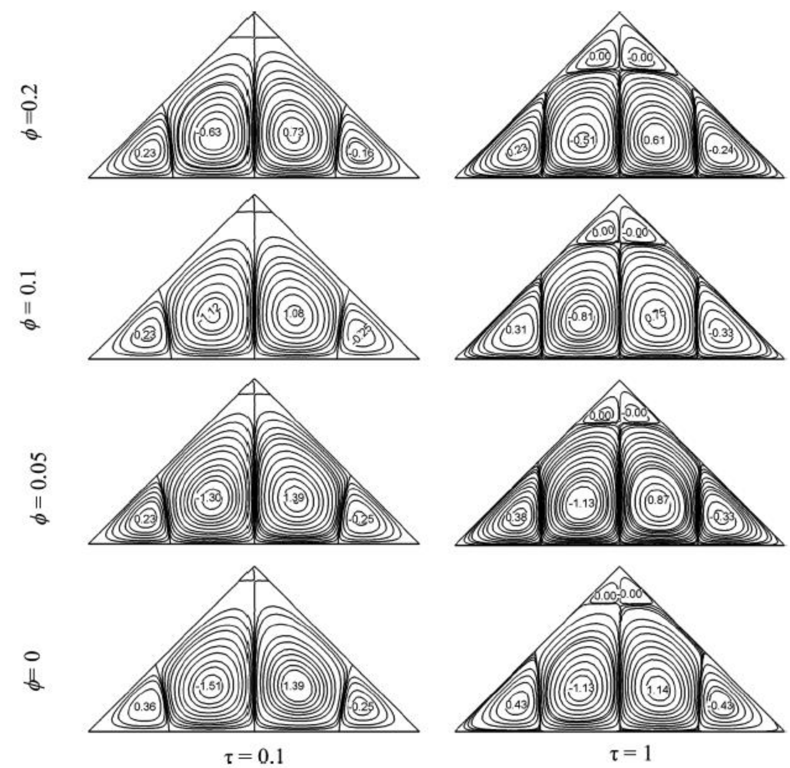

Figure 5. Effect of solid volume fraction on streamlines for the selected values of τ with $Ra = 10^6$ (CuO-water).

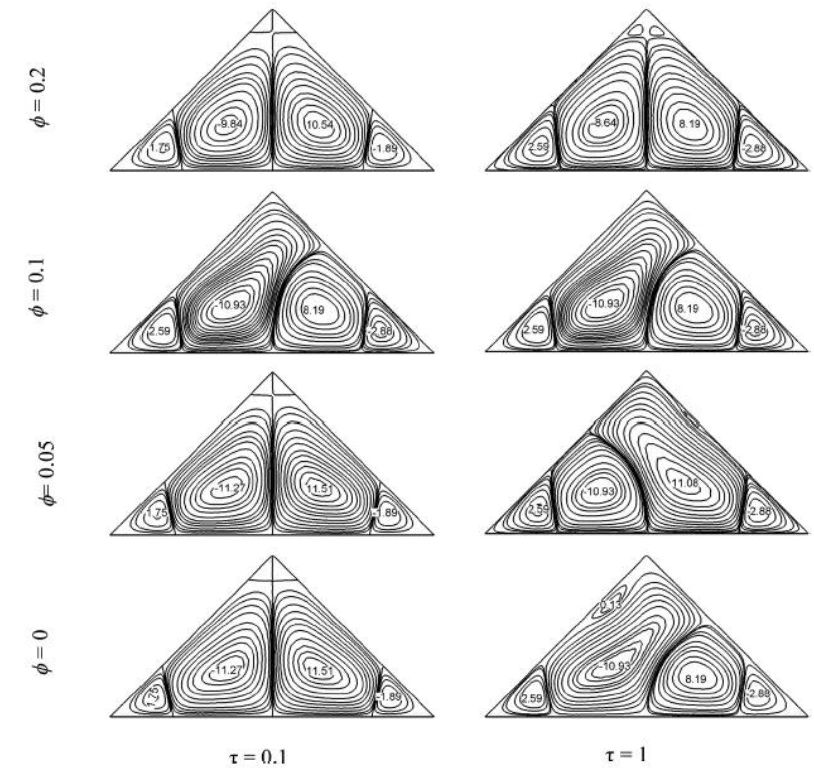

Figure 6. Effect of solid volume fraction on streamlines for the selected values of τ with $Ra = 10^7$ (CuO-water).

Ra obviously increase the intensity of convection. However, the most interesting point here is to observe how the amount of nanoparticles affects the convection.

There is a very obvious pattern in the formation of vortices inside the enclosure for every case at $\tau = 0.1$ and for $Ra = 10^5$ to $Ra = 10^7$. There are more or less always four cells formed in a symmetric manner. Two larger cells are near the middle of the enclosure and have comparable strengths. However, they rotate opposite to each other. Besides these two primary cells, there are two other symmetrically formed secondary cells or eddies at the two corners near the bottom wall. The convective streamline pattern is due to the boundary conditions which have been applied to the enclosure. Since $\tau = 0.1$, which means the process is still in its initial stage, the vortices are still not stabilized and hence almost always have a higher value of streamfunction than that of $\tau = 1$. Another important change in the streamline patterns is that there are two smaller cells at the top of the enclosure with opposite sense of rotation, and these cells are very weak. First, if the reason for this streamline pattern is investigated, it would be apparent that the boundary condition (temperature) at the heated bottom wall is a sine-squared function, which indicates that, along the boundary line, the temperature will reach its peak twice and there will be a base in between. As a result, two major cells are formed inside the enclosure. And the strong local convection results in the two eddies that can be seen near the corners.

Link to Full-Text Articles :

http://www.tandfonline.com/doi/pdf/10.1080/10407790.2014.992058 *http://www.ingentaconnect.com/content/tandf/unhb/2015/00000068/00000001/art00004*